UCRL - 74345 Rev. 1
PREPRINT

CONF-730836--2

LAWRENCE LIVERMORE LABORATORY
University of California / Livermore, California

LASER INDUCED IMPLOSION AND THERMONUCLEAR BURN

John H. Nuckolls

July 23, 1973

This is an invited paper prepared for presentation at
3rd Laser Interaction Workshop-Conference,
Rensselaer Polytechnic Institute, August, 1973.

LASER INDUCED IMPLOSION AND THERMONUCLEAR BURN*†

John H. Nuckolls
University of California Lawrence Livermore Laboratory

In high density laser induced fusion, the key idea is laser implosion of hydrogen isotope microspheres to approximately 10,000 times liquid density in order to initiate efficient thermonuclear burning[1]. Fusion yields 50-100 times larger than the laser energy for laser energies of 10^5-10^6 joules have been achieved in sophisticated computer simulation calculations. Most of the dense pellet is isentropically compressed to a high density Fermi-degenerate state, while thermonuclear burn is initiated in the central region. A thermonuclear burn front propagates radially outward from the central region heating and igniting the dense fuel.

The laser fusion implosion system consists of a tiny spherical pellet of deuterium-tritium surrounded by a low density atmosphere extending to several pellet radii, located in a large vacuum chamber, and a laser capable of generating an optimally shaped pulse of light energy. Figure 1. The atmosphere may be produced by ablating the pellet surface with a laser prepulse. Mirrors (or lenses) are used to focus the laser light on the

*Work Performed Under the Auspices of the U.S. Atomic Energy Commission.

†Revised version of UCRL-74345 (1972) same title (invited paper presented at APS meetings at Los Angeles, Dec., 1972; New York, Jan., 1973, and Hartford, Apr., 1973).

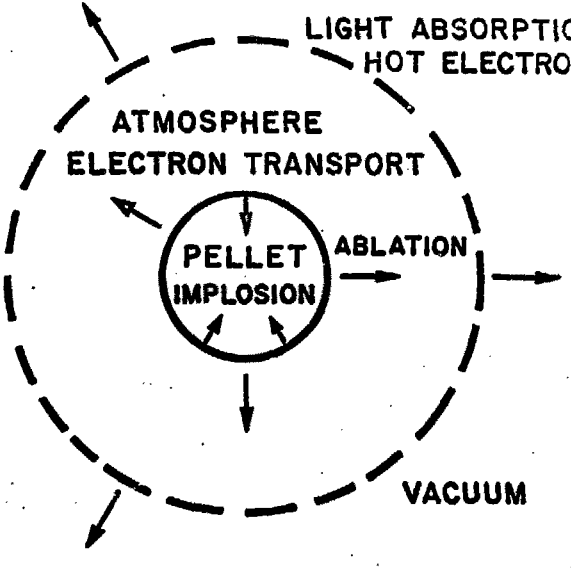

Figure 1

Important features of the laser implosion system

atmosphere more or less uniformly from all sides. Absorption of the laser light in the outer atmosphere generates hot electrons. The atmosphere and the pellet surface are heated by electron diffusion and transport. As the electrons move inward through the atmosphere, scattering and solid angle effects greatly increase the spherical symmetry. Violent ablation and blowoff of the pellet surface generates the pressures which implode the pellet. This is essentially a spherical rocket. The laser pulse is shaped (in time) to achieve ultra-high compressions of the pellet while fully exploiting electron degeneracy and thermonuclear propagation to maximize the fusion yield.

THERMONUCLEAR BURN

The feasibility of thermonuclear explosions was demonstrated by Los Alamos scientists in the early 1950's [2].

Thermonuclear micro-explosions scale as the density-radius product ρR. The rates of burn, energy deposition by charged reaction products, and electron-ion heating are proportional to the density, and the inertial confinement time is proportional to the radius. Consequently the burn efficiency, self-heating, and feasibility of thermonuclear propagation are determined by ρR. In spherical compression, ρR increases (because $\rho \propto R^{-3}$) and is proportional to $(M\rho^2)^{1/3}$, where M is the mass. Compression by 10^4 reduces the mass--and laser energy--required to initiate an efficient thermonuclear micro-explosion by up to 10^8-fold, depending on the efficiency of the compression process.

The burn efficiency, ϕ, is proportional to the product of the burn rate, $\overline{\rho\sigma v}$, and the inertial confinement time, $\frac{R}{4C}$, where $\overline{\sigma v}$ is the Maxwell velocity-averaged reaction cross section and C is the sound speed. The factor of 4 arises because in a sphere half the mass is beyond 80% of the radius. Both $\overline{\sigma v}$ and C depend on temperature, but their ratio is approximately constant in the 20-50 keV temperature range characteristic of efficient deuterium-tritium micro-explosions. Using $\frac{\overline{\sigma v}}{C}$ evaluated at 20 keV, and correcting for depletion, it follows that [3]

$$\phi \approx \frac{R\rho}{6+R\rho}$$

At $\rho R = 3$ g/cm^2, $\phi \gtrsim \frac{1}{3}$, corresponding to a fusion energy release of $\sim 10^{11}$ joules/g.

The average specific heat energy required for ignition is

$$C_p \theta_{ign} \beta$$

where C_p is the heat capacity, θ_{ign} is the ignition temperature, and β is a correction for the self-heating by the 3.6 MeV DT alpha particles, and for thermonuclear propagation.

If $\rho R \gg 0.3$ g/cm^2, then only about 0.3 g/cm^2 in the central region need be heated to approximately 10 keV in order to initiate a radially propagating burn front which ignites the entire pellet. In this case 1.6×10^{10} joules/g of fusion energy will be released from the central region; one fifth of the energy is in alpha particles, sufficient to heat 3 times more DT to 10 keV. The alpha particles will deposit their energy in approximately this mass since their range in 10 keV DT is about 0.3 g/cm^2.

Due to the effects of shock convergence and pulse shaping during implosion, the DT temperature just prior to ignition may be made to vary approximately as R^{-2}. Then β is proportional to $(\rho R)^{-2}$. Because of practical limitations on implosion symmetry, a minimum of ~ 0.03 is imposed on β, which occurs for $\rho R \geq 3$ g/cm^2. Then the average ignition energy is 3×10^7 joules/g. This is also the minimum compressional energy of DT at a density of 1000 g/cm^3, and this minimum occurs if the DT electrons are Fermi-degenerate[4]:

$$\varepsilon = \varepsilon_F \left[\frac{3}{5} + \frac{\pi^2}{4}\left(\frac{\theta_e}{\varepsilon_F}\right)^2 + \ldots\right]$$

where ε_F, the Fermi-energy, is $\frac{h^2}{8m}\left(\frac{3}{\pi} n_e\right)^{2/3}$, h is Planck's constant, m is the electron mass, θ_e is the electron temperature, and n_e is the electron density. For $\rho = 1000$ g/cm^3 ($n_e \approx 2.5 \times 10^{26}$/cm^3), $\varepsilon_F \approx 1$ keV, and the DT electrons are degenerate if the implosion is carried out so that $\theta_e \ll 1$ keV (except in the central region where ignition occurs).

The minimum average energy of ignition and compression with $\rho R \sim 3$ g/cm^2, assuming propagation and degeneracy, is roughly the sum of the compression and ignition terms, or $\sim 6 \times 10^7$ joules/g. Since the fusion energy produced at this ρR is 10^{11} joules/g, the gain is ~ 1500. Approximately 95% of the laser energy absorbed by the pellet during implosion is lost to kinetic and internal energy of the blowoff. Consequently the energy gain relative to the laser light employed is about 75 fold. This is sufficient for CTR applications with a 10% efficient laser, a 40% thermal-to-electric efficiency, and about 30% of the electrical energy circulated internally.

Figure 2 shows the variation of gain (relative to laser light energy) with compression and laser light energy[16]. The curves have been slightly normalized to computer calculations of the implosion and burn. Gains approaching 100 are predicted for laser energies of 10^6 joules. The calculations indicate that less than 1 kJ of laser light may be sufficient for breakeven (gain ≈ 1) and 10^5 joules may be sufficient to generate net electrical energy with a 10% efficient laser. These predicted gains are probably upper limits to what can be achieved. Unforeseen difficulties may cause significant performance degradations when the predictions are experimentally tested.

Similar gain curves may be generated for D_2, DHe^3, and $B^{11}p_x$ pellets seeded

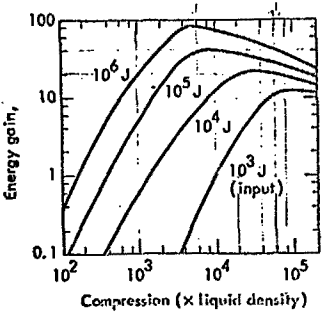

Calculated gain (ratio of fusion energy output to laser light energy input) as a function of fuel compression η for several different laser light energy inputs. At compressions less than about 10^3, the gain increases strongly with increasing compression because of increasing burn efficiency and propagation. The gain decreases with compressions much greater than 10^4 because of depletion of the DT and because the energy of compression (against degeneracy pressures) becomes dominant.

FIGURE 2

with a small percentage of tritium to facilitate ignition. Since these reactions have smaller $\overline{\sigma v}$'s than DT, higher ρR's are required for efficient burn. This may be achieved either by use of larger pellets and higher energy lasers, or by compressing the pellet to higher densities ($\sim 10^4$ g/cm^3). The D_2 and DH^3 fuels produce fewer neutrons than DT, and the $B^{11}p_x$ fuel produces essentially no neutrons[5].

IMPLOSION

Conditions involving pressure, symmetry, and stability must be satisfied in order to implode a DT sphere to a state at 10^4 times liquid density, in which both Fermi-degeneracy and thermonuclear propagation can be exploited to achieve maximum gain[1]. A pressure of at least 10^{12} atmospheres must be generated. Much higher pressures are required if the electrons in the high density DT are not Fermi-degenerate, i.e. if the implosion is not essentially isentropic. The pressures applied to implode the pellet must be uniform spatially and temporally to less than one part in twenty in order to preserve effective spherical symmetry. During compression the radius decreases by about 20-fold ($10{,}000^{1/3}$), and it is necessary to maintain sufficient symmetry within the central region in order to utilize central ignition and propagation. The hydrodynamic Rayleigh-Taylor instability must be controlled. Otherwise the pellet surface cannot be relatively gradually accelerated during the implosion as required by the optimum pulse shape. These conditions may be satisfied by the characteristics of the laser pulse shape and of the laser implosion scheme.

Pressure

The minimum pressure of DT at 10^4 times liquid density is 10^{12} atmospheres, and occurs if the electrons are Fermi-degenerate. If $\theta \approx 5$ keV, the ideal ignition temperature for DT, the electrons are not degenerate, and the pressure is 10^{13} atmospheres. The required 10^{12} atmosphere pressure is generated by focussing the high power laser light to high intensities on the outer atmosphere, multiplying the absorbed energy flux by electron transport in the spherically convergent density gradient from the outer atmosphere to the pellet surface, ablating the pellet surface, and multiplying the resulting ablation pressures by the concentration of energy density which occurs in the implosion process.

Absorption. Laser light is focussed to intensities as high as 10^{15} watts/cm^2 on the outer atmosphere. Absorption occurs at densities less than the critical density (where the plasma frequency equals the optical frequency) by inverse bremsstrahlung and by plasma instabilities if the intensity exceeds the instability thresholds. Figure 3 from Shearer[6] shows the inverse bremsstrahlung opacity in matter at one keV temperature for Nd laser light ($\lambda \approx 10^{-4}$cm). The light slows down as it approaches the critical density (10^{21} electrons/cm^3 for Nd light), the electromagnetic field increases, and at high intensities the quivering velocity of the electrons may exceed their thermal velocity. The inverse bremsstrahlung opacity scales as follows:

$$K_{\text{inverse brem}} \sim \frac{Z^3}{A^2} \frac{n^2}{(1-n/n_c)^{\frac{1}{2}}} \lambda^2 \theta_e^{-3/2} \text{ cm}^{-1}$$

where θ_e is the electron temperature, λ is the laser wavelength, n is the electron density, n_c is the critical electron density ($\sim \lambda^{-2}$), A is the atomic weight, and Z is the effective charge. Since in typical laser fusion pellets the scale height of density is comparable to one mm, efficient absorption via inverse bremsstrahlung is not possible with Nd at electron temperatures $\gtrsim$ 10 keV, or with CO_2, at electron temperatures $\gtrsim$ 1 keV. Plasma simulation calculations show that the instability absorption length near the critical density is approximately ten wavelengths[7], or 10^{-3}cm for Nd light. The threshold for the modified two-stream instability is approximately[7]

$$\text{Instability threshold} \sim \left(\frac{n_c}{\theta_e}\right)^{\frac{3}{4}} Z \times S$$

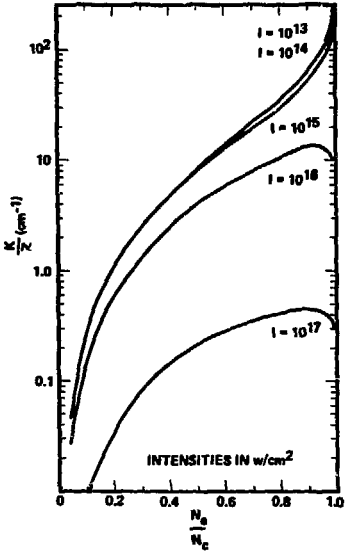

FIGURE 3

Inverse bremsstrahlung opacity f laser light absorption, 1 μm wavelength, one keV electron temperature[6].

where the swelling factor, S, corrects for the increasing electromagnetic field as the light approaches the critical density. For 1 keV DT, this threshold is approximately 10^{12} watts/cm^2.

Electron Spectrum. Absorption of intense laser light generates hot electrons. If absorption is by inverse bremsstrahlung the electron spectrum is near Maxwellian

$$f(v_e)_{\text{inverse brem}} \sim v_e \exp\left(-\frac{Mv_e^2}{2\theta_e}\right)$$

where v_e is the electron velocity. If absorption is by plasma instabilities the electron spectrum may be non-Maxwellian[8]. Figure 4 shows an electron spectrum calculated by a plasma simulation computer program[8]. An exponential-like tail extends to 100 times the thermal electron energy.

The laser heated electrons heat the pellet atmosphere by electron-electron collisions. The mean free path, λ_{e-e}, is

$$\lambda_{e-e} \sim E_e^2 n^{-1}$$

$$\sim 1 \text{ cm}, E_e \sim 60 \text{ keV}, n \sim 10^{21} \text{ cm}^{-3}.$$

where E_e is the electron energy. After a tiny fraction of the electrons escape into the vacuum chamber, electrostatic potentials comparable to θ_e are generated and the remaining electrons are trapped within the atmosphere which expands at ion velocities. Sufficiently high energy electrons will reflect back and forth across the atmosphere many times before losing a significant fraction of their energy.

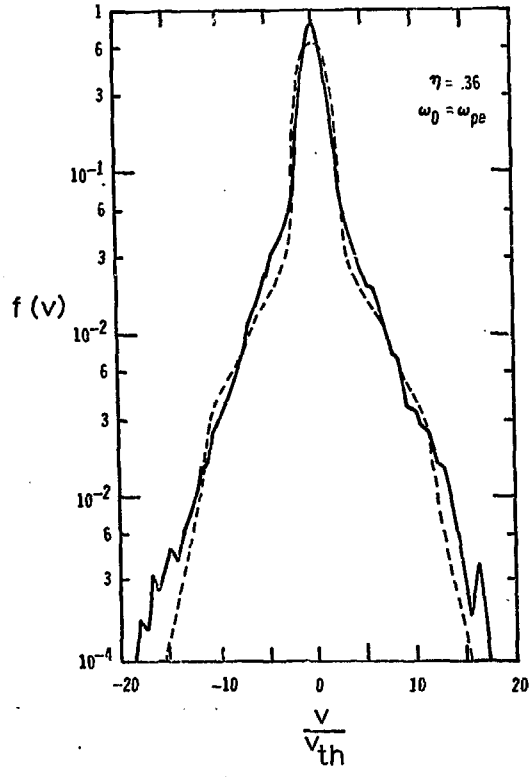

FIGURE 4

Calculated electron spectra generated by absorption of intense laser light via plasma instabilities; v electron velocity, v_{th} thermal electron velocity.

Ablation Pressure. Typically the density falls off inversely as radius cubed from the ablating radius to the absorption radius. So long as electron-electron collisions are sufficiently rapid energy is strongly coupled by electron transport in this spherically convergent gradient from the absorbing surface to the much smaller ablating surface. Then

$$\dot{E} \approx 2\, P_A C A_p + \text{smaller terms}$$

where P_A is the ablation pressure, A_p is the ablating surface area, the factor 2 corrects for heating of the blowoff--through which energy is transported, and $\dot{E}$ is the absorbed laser power. The blow-off velocity, C, is approximately sound speed in the hot atmosphere

$$C \approx \sqrt{\frac{P}{\rho}} \sim \theta_e^{\frac{1}{2}}$$

where θ_e is the electron temperature. This temperature is determined largely by the equation for flux limited electron transport

$$n_c\, v_e\, \Delta E\, A_c \approx \dot{E}$$

where $n_c\, v_e$ is the incident electron flux, ΔE is the net energy carried by each electron from the absorption region, and A_c is the absorption area. Then it follows that the ablation pressure is approximately

$$P_A \approx \frac{A_c}{A_p} \left(\frac{\dot{E}}{A_c}\right)^{2/3} \rho_c^{1/3}$$

where ρ_c is the critical density in g/cm^3. If $A_c = A_p$ (plane geometry) this is the equation derived by Kidder[9]. The pressure is multiplied by a factor A_c/A_p by electron transport in the convergent density gradient.

The ablation coupling efficiency is

$$\frac{P_A A_p}{\dot{E}} \approx \frac{v}{2C}$$

where v is the implosion velocity. Typically v varies from 10^6 to 3×10^7 cm/s while C varies from 2×10^7 to 10^8 cm/s, so that the coupling efficiency varies from 2 to 15 percent. Most of the energy is coupled near the end of the implosion, so that the average coupling efficiency is 5-10 percent.

Decoupling. If the hot electron range becomes comparable to the absorption radius, the electron may cross the pellet, re-enter the region in which laser light is absorbed and be further heated before its energy is lost to colder electrons. Then the electrons are heated to even higher energies, have a larger range, and lose energy even more slowly to the colder electrons[10]. The threshold for onset of this decoupling determines a maximum hot electron energy and laser intensity, and thereby a maximum ablation pressure:

$$P_{max} \approx 10^2 \frac{A_c}{A_p} A_c^{\frac{1}{4}} \rho_c^{3/2}$$

However if the density gradient is steeper than R^{-3}, (as in implosion of hollow pellets), higher pressures may be generated. Decoupling is a serious problem for CO_2 laser implosions, and weakly effects Nd laser implosions. For larger pellets and laser energies decoupling becomes less severe because the hydrodynamic time is larger. Decoupling can be compensated for if the initial volume is increased by making the pellet hollow. Then the required implosion velocity may be achieved with limited implosion pressures (acting over a larger volume).

Preheat. Electrons with energies of 50 keV have a range of 100 μ in liquid density DT, comparable to the thicknesses of typical laser fusion pellets. Electrons of this energy are generated by long wavelength lasers even if the electron spectrum is assumed to be Maxwellian because of decoupling effects and by lasers of any wavelength via instabilities if non-Maxwellian electron spectra are assumed. If the flux of these electrons is too high the resulting preheating may make compression to a Fermi-degenerate state impossible, and high compression extremely difficult[1]. The tolerable fraction of electron energy in hot electrons with range comparable to the pellet thickness is exceeded when the preheat energy flux is comparable to the implosion energy flux:

$$f \approx \frac{P_A v}{P_e v_e}$$

where P_A is the ablation pressure, v is the implosion velocity, P_e is the electron pressure, and v_e the hot electron velocity. In the initial stages of a CO_2 implosion P_A is 1 Mb and v is 1 cm/μs, while P_e is 10^{-2} Mb ($\theta_e \sim \frac{1}{2}$ keV) and v_e is 10^4 cm/μs, so that f is only one percent. For Nd f is initially 10^{-2}%. Because of the preheat problem, absorption of the laser light by plasma instabilities may not be feasible for some laser fusion pellet designs. Since high intensity CO_2 light must be absorbed by instabilities, it is possible that CO_2 is not suitable for high density laser fusion. In order to increase the instability threshold and the inverse bremsstrahlung opacity, seeding of the pellet with ~ 0.1 atom % of high Z material, and use of short wavelength lasers is advantageous. The instability threshold may also be increased by frequency modulation of the laser.

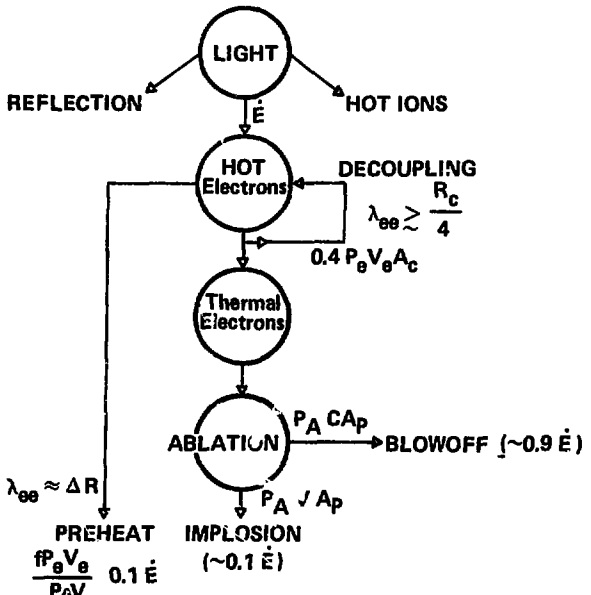

FIGURE 5

Modes of energy transfer and coupling in laser implosion.

Magnetic Field. Spontaneous magnetic fields are generated due to the non-uniform irradiation of the atmosphere with the laser[11]. Gradients in the electron pressure and in the electron density are generated which have a non-zero cross product (via the electron temperature). Then[12]

$$\vec{B} \propto \nabla \times \left[\vec{v} \times \vec{B} + \frac{c}{en_e} \nabla P_e + \cdots\right]$$

Implosion calculations with ion wavelength lasers (e.g. CO_2) show magnetic fields sufficiently large to inhibit electron transport. However the magnetic energy density is much smaller than the electron energy density. The effect of the magnetic field may be reduced by increasing the collision frequency (via short wavelength lasers and seeding with small amounts of high Z material).

Implosion. In the implosion the applied ablation pressure first generates kinetic energy

$$\bar{P}_A (V_o - V_f) \propto \frac{1}{2} M v^2$$

where $\bar{P}_A$ is the average ablation pressure, V_o is the initial volume, and V_f is the final volume. At maximum compression most of this kinetic energy is internal, so that the pressure multiplication ratio is proportional to the compression

$$P_{max} \approx (\gamma-1) \frac{\frac{1}{2} M v^2}{V_f} \approx (\gamma-1) \frac{\bar{P}_A (V_o - V_f)}{V_f}$$

$$\therefore \quad \frac{P_{max}}{\bar{P}_A} \approx (\gamma-1) \frac{V_o}{V_f}, \quad V_o \gg V_f$$

Convergence transforms the kinetic to internal energy nearly isentropically--except for a small region near the implosion center. If the matter is compressed to a Fermi-degenerate state (the initial implosion velocity is near sonic and the subsequent ablation pressure increases sufficiently gradually) then

$$P \sim \rho^{\gamma}, \ \gamma \approx \frac{5}{3}$$

and

$$\left(\frac{P_{max}}{\bar{P}_A}\right) \approx \left(\frac{\bar{P}_A}{P_{Ao}}\right)^{3/2} \left(\frac{2}{3} V_o \frac{\rho_o}{M}\right)^{5/2}$$

where P_{Ao} is the initial ablation pressure.

Large pressure multiplications may be achieved even if $\bar{P}_A$ is limited (e.g. by decoupling) by use of hollow pellets (V_o term). However V_o cannot be made indefinitely large because of symmetry and stability constraints. The multiplication ratio is also increased by making the average ablation pressure large compared to the initial pressure (via pulse shaping). Because of the magnitude of the Fermi-energy in matter under ordinary conditions, the entropy is not significantly decreased by making P_{Ao} much less than one half megabar.

Pulse Shape. The optimum laser pulse shape--which maximizes the fusion yield for a given laser energy--satisfies five conditions.

(1) Densities greater than 1000 g/cm^3 are achieved.

(2) The implosion occurs in less than one sonic transit time so that long wavelength Taylor unstable growth is tolerable.

(3) In most of the compressed pellet the electrons are Fermi-degenerate. This minimizes the laser energy required for compression.

(4) The central core of the compressed pellet--having a radius comparable to the DT alpha range--reaches temperatures of $\sim$ 10 keV, initiating rapid thermonuclear burn and propagation. This minimizes the laser energy required for ignition.

(5) The implosion and blowoff velocities are increased together so as to maximize the ablation efficiency.

These five conditions are satisfied by a pulse shape having the following two properties.

(1) The initial implosion velocity is $\sim$ 1 cm/μs, slightly larger than sound speed. This shock is sufficiently weak so that most of the pellet can be compressed to a Fermi-degenerate state, but--with convergence--is strong enough so that the center is significantly shock heated. The peak implosion velocity is sufficiently large ($\gtrsim$ 3 x 10^7 cm/s) so that densities of 1000 g/cm^3 are reached, and central ignition occurs.

(2) The implosion pressure is increased with time so that the hydrodynamic characteristics coalesce within most of the compressed mass, but beyond one alpha particle range from the center. This insures isentropic Fermi-degenerate compression of most of the pellet while igniting the central region.

By means of hundreds of implosion/burn computer calculations, the optimum pulse shape (laser power history) has been determined. In these calculations the pulse shape was represented by an eight element histogram. The amplitudes and durations of the elements were varied to optimize the ratio of fusion energy to laser light energy. For solid DT pellets in which preheat, decoupling, and other effects are not important, the optimum histogram can be approximated by the following equation:

$$\dot{E} = \dot{E}_0 \tau^{-s}, \text{ where } \tau = 1 - \frac{t}{t'}, \; t < t'$$

$$s \approx \frac{3\gamma}{\gamma+1} \approx 2 \text{ (if } \gamma = \frac{5}{3}\text{), and } \gamma = \frac{pV}{\varepsilon} + 1.$$

where $\dot{E}_0$ is the initial laser power (which generates an initial implosion velocity of $\sim$ 1 cm/μs), and t' is the transit time (to the center) of the initial shock.

If the pellet is hollow or seeded, or if preheat, decoupling, or other effects are important, the optimum pulse shape is significantly modified. Symmetry requirements also affect the optimum pulse shape.

Symmetry

In compression of a sphere by 10^4-fold, the radius decreases somewhat more than 20-fold. If after compression spherical symmetry is required to within 1/2 the compressed radius (1/40 the initial radius) then the implosion velocity (and time) must be spatially uniform (and synchronized) to $\sim$ one part in 40, or a few percent[1]. In general, for a spherical implosion in which the ratio of initial to final volumes is η, and in which the tolerable error in the final radius, R, is wR, the tolerable fractional error in the integral of velocity and time is approximately

$$\frac{\Delta \int v dt}{\int v dt} \simeq \frac{w}{\eta^{1/3}}, \quad \eta >> 1.$$

Implosion errors may be reduced to about 10% by a many-sided irradiation system, consisting of a laser, beam splitters, mirrors, lenses, and other optical elements. This error can then be reduced to less than 1% by means of electron transport in the atmosphere surrounding the pellet.

Multiple Beam Irradiation. If a sphere is irradiated from all sides with many laser beams focussed to the diameter of the sphere, intensity variations over the spherical surface as small as 10% may readily be achieved. However light which is not incident perpendicular to the spherical surface is refracted in the density gradient[6]. If the incident angle is more than 30^0 from normal, the light trajectory in the density gradient does not not approach the critical density surface. Then absorption by plasma instabilities is not possible. Also absorption by inverse

bremsstrahlung occurs at low densities, so that the electron decoupling problem is more severe.

Using f/1 optics the entire surface of a sphere cannot be illuminated by as few as six circular laser beams focussed on the center of the sphere. However if each of six beams is focussed to a point one spherical radius beyond the center (along the axis of each beam) then the entire surface is illuminated, and the maximum angular deviation from normal incidence is less than twenty degrees. If the overlapping edges of the beam are blocked (so that each beam is four sided instead of circular) then the maximum error in intensity of illumination is 10-20%. This error may be reduced to less than 10% by using more laser beams, e.g. 12 beams with pentagonal cross section.

Complex lenses and mirrors may also be used to increase the symmetry of irradiation.

Electron Transport in Atmosphere. The region in the atmosphere where the laser light is absorbed has a radius several times that at which ablation occurs. Consequently each point on the ablating surface is heated by nearly 2π steradians of the absorbing region. If many laser beams are used, e.g. 12 pentagons, then each beam occupies a small fraction of 2π steradians, and each point on the ablating surface is effectively heated by many beams. These effects reduce the irradiation error.

The range of the laser heated electrons in the low density region where the laser light is absorbed is comparable to the diameter of one of the multiple focussed laser beams, and is also a significant fraction of

the radius of the absorbing region during most of the implosion. Hence non-uniformities which occur over small areas are strongly smoothed. In addition there are many electron scattering mean free paths through the density gradient between the absorbing and ablating surfaces. The smoothing due to scattering during electron transport may be estimated by use of spherical harmonic analysis if a steady state, a short electron mean free path, and a uniform density are assumed[13]. This analysis shows that scattering in the atmosphere reduces the heating error from 10-20% at the absorbing surface to less than 1% at the ablating surface with heating by eight laser beams. Solution of this problem with the real (non-uniform) density gradient would reduce the heating errors even further.

Stability

The unstable growth of small surface perturbations during acceleration of a fluid interface is described by the Rayleigh-Taylor theory[14].

$$A = A_0 e^{\int \sigma dt}, \quad \sigma^2 = aK$$

where A_0 is the initial amplitude of a perturbation with wavenumber K, and a is the acceleration. Unless some stabilization mechanism can be utilized, a fluid shell can be accelerated through only about five thicknesses before it is essentially destroyed by this instability. However in the laser fusion implosion scheme described here the optimum pulse shape may accelerate shells through many tens of thicknesses. Stabilization is achieved by several means.

(1) Growth of perturbations with wavelength less than $\sim 2\pi$ times the shell thickness is prevented because the implosion pressure is generated by surface ablation driven by diffusing electrons. Under these conditions

$$\sigma^2 = aK - \frac{P_A K^2}{\rho}$$

where P_A is the ablation pressure[15]. This stabilizing effect occurs largely because the temperature gradient near the peak of the perturbation is steeper than the gradient near the valley. Consequently the rate of transport of energy is higher to the peak than to the valley, and higher ablation rates and ablation pressures are generated. This reduces the amplitude of the perturbation.

(2) Growth of long wavelength perturbations--which have a slower growth rate--is sufficiently limited by imploding the pellet as rapidly as possible consistent with compression to a Fermi-degenerate state. Consequently the initial implosion velocity is somewhat supersonic.

(3) Pellets are used which have an initial ratio of shell thickness to radius to more than 2%. If thinner shells are used, perturbations with wavelengths greater than 2π times the shell thickness (which are not stabilized by ablation) grow so large that the shell is destroyed.

COMPUTER CALCULATIONS

The compression and burn processes which have been described are illustrated in results of a typical computer simulation calculation of the implosion of a fusion pellet to 10,000 times liquid density, and of the resulting thermonuclear micro-explosion. This calculation was carried out at the Livermore Laboratory by Albert Thiessen on the CDC 7600 computer with the LASNEX program developed by George Zimmerman[16]. LASNEX is a two-dimensional (axially symmetric) finite difference code which includes models of the following physical processes (Figure 6)

Hydrodynamics--Lagrangian; real and generalized Von Neumann artificial viscosities; pondermotive, electron, ion, photon, magnetic, and alpha particle pressures.

Laser light--absorption via inverse bremsstrahlung and plasma instabilities; reflection at critical density.

Coulomb coupling of charged particle species.

Suprathermal electrons--Multigroup flux-limited diffusion with self-consistent electric fields; non-Maxwellian electron spectra determined by results of plasma simulation calculations for laser light absorption by plasma instabilities; inverse bremsstrahlung electron spectrum for classical absorption.

Thermal electrons and ions--flux-limited diffusion.

Magnetic field--includes modification of all charged particle transport coefficients, as well as most of the equilibrium MHD effects described by Braginskii[12].

LASNEX PHYSICS

FIGURE 6

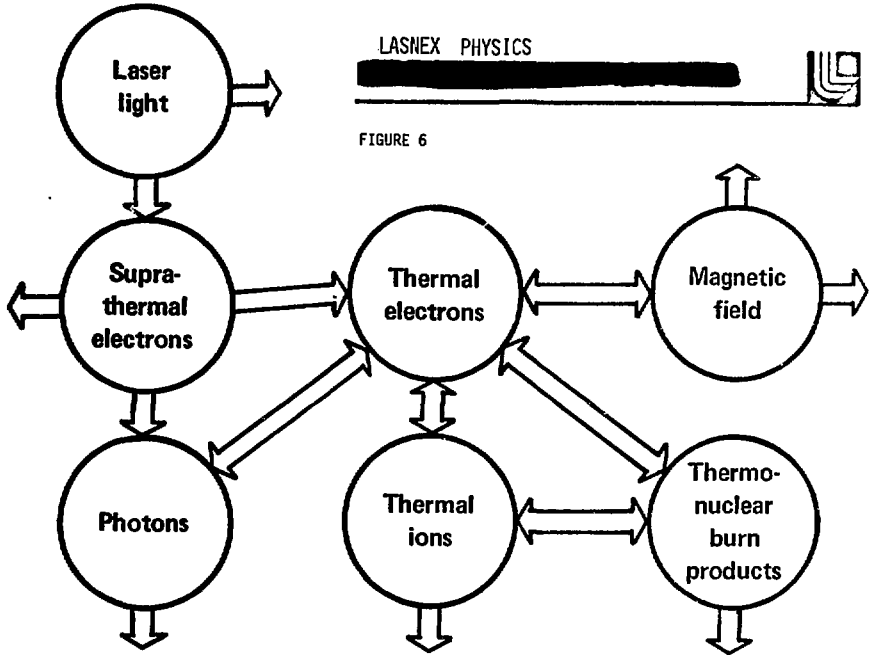

Physical processes modelled in the LASNEX laser implosion/fusion computer program.

Photonics--Multigroup flux-limited diffusion[17]; LTE non-LTE average-atom opacities for free-free, bound-free, and bound-bound processes[18]; Fokker-Planck treatment of Compton scattering[19].

Fusion--Maxwell velocity-averaged reaction rates; the DT alpha particle is transported by a one group flux-limited diffusion model with appropriate energy deposition into the electron and ion fields; one group transport of the 14 MeV neutron.

Material properties--opacities, pressures, specific heats, and other properties of matter are used which take into account nuclear Coulomb, degeneracy, partial ionization, and other significant effects.

In this implosion calculation, a 60 KJ, short wavelength ($\lesssim \frac{1}{2}$ μ), frequency-modulated, pulse of laser light is focussed symmetrically onto a 1200 μm radius low density atmosphere (generated by a laser prepulse) surrounding a 400 μm radius spherical pellet of liquid deuterium-tritium. The applied laser power is increased in 8 pulses from $\sim 10^{11}$ to $\sim 10^{15}$ watts in 10 nanoseconds. These 8 pulses closely approximate the ideal pulse shape described earlier. The laser light is absorbed via inverse bremsstrahlung and plasma instabilities near the critical density in the atmosphere, at a radius of approximately 600 μm, generating hot electrons. The pellet and atmosphere are seeded with small amounts of material of $Z \gg 1$ (and short wavelength laser light is used) in order to make possible efficient absorption by inverse bremsstrahlung, and in order to increase the thresholds for plasma instabilities. Frequency modulation of the laser light also increases the instability thresholds[20]. When these effects are accounted for, the peak laser intensity is less than a factor of ten above the threshold

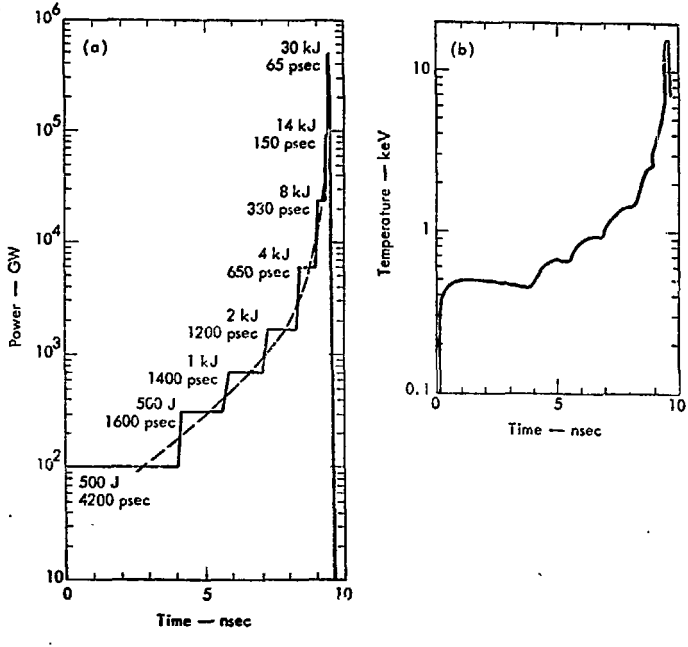

Computer calculations of a 10,000-fold compression of a fusion pellet and the resulting thermonuclear microexplosion. (a) Laser pulse power rises in steps to approximate ideal pulse shape shown by dashed curve. (b) Corresponding electron temperature in critical density region.

Figure 7

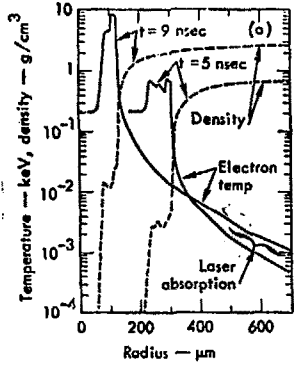

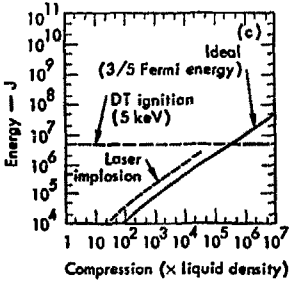

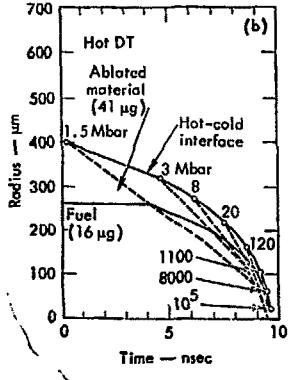

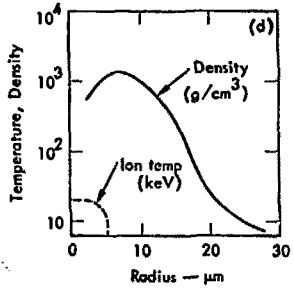

Computer calculations (continued) of a 10,000-fold compression of a fusion pellet and the resulting thermonuclear microexplosion. (a) Density and electron temperature vs radius at times of 5 and 9 nsec. (b) Radius vs time (dashed lines are weak shocks from steps in pulse power, implosion pressures are shown in megabars). (c) Typical calculated laser implosion isentrope and ideal isentrope. (d) Density and electron temperature vs radius at ignition.

Figure 8

for instabilities--so that generation of strongly non-Maxwellian electron distributions is avoided. The atmosphere is heated by the hot electrons to electron temperatures which increase in time from $\sim 3 \times 10^6$ to 10^8 ^oK at the absorption radius. The surface of the pellet is heated and ablated by electron thermal conduction through the hot atmosphere, generating implosion pressures which optimally increase from $\sim 10^6$ to $\sim 10^{11}$ atmospheres. This five order of magnitude increase in implosion pressure occurs at an optimal rate during transit of the initial shock to the center. Consequently the outer part of the pellet is isentropically compressed into a high density spherical shell ($\rho > 100$ g/cm^3) while at the same time this shell is inwardly accelerated to velocities which increase in time from 10^6 to 3.5×10^7 cm/s. As the internal pressure becomes larger than the ablation pressure the rapidly converging shell slows down and is compressed near isentropically, at sub-Fermi-temperatures, to densities greater than 1000 g/cm^3. The inner region is compressed by the outer shell to densities approaching 1000 g/cm^3, and heated to ion temperatures greater than 10^8 ^oK, initiating thermonuclear burn. A thermonuclear burn front then propagates outward. About 1200 KJ of fusion energy is produced in less than 10^{-11} seconds. The energy gain is about 20 fold.

Figure 9 shows the structure of the outwardly propagating thermonuclear burn front. Compression is about 2 fold. The matter velocity defines a flame front and peaks at 10^8 cm/s. In the center of the pellet the ion temperature exceeds the electron temperature, but in the burn front there is an electron temperature precursor. This is mainly due to the alpha particles which deposit most of their energy in electrons at 10 keV electron temperatures and equally in ions and electrons at 30-40 keV, and to the cooling of the electrons by thermal conduction and bremsstrahlung.

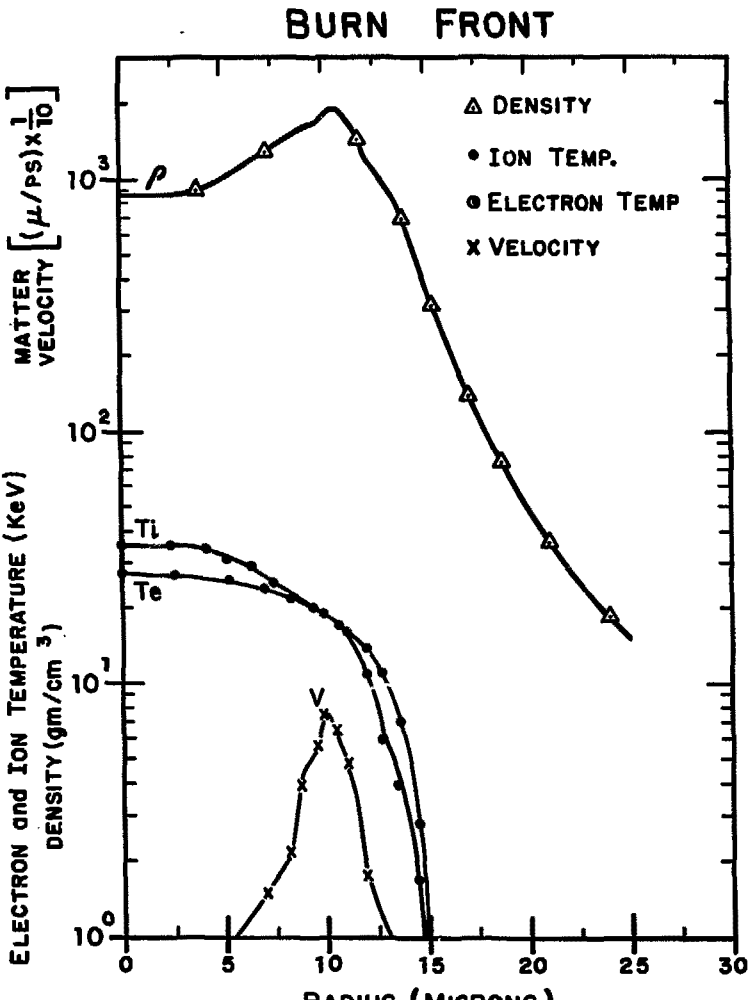

FIGURE 9

Structure of thermonuclear burn front

A two-dimensional calculation has been made of a similar pellet configuration to study symmetry and Taylor instability. This calculation was made on the LASNEX code by A. Thiessen and G. Zimmerman. The initially spherical pellet was irradiated with ten laser beams consisting of adjacent equiangular (18^0) conical shells symmetric about a common axis. The laser intensity varied sinusoidally ± 10% across each beam. Frequency modulation was assumed and the laser wavelength was varied from 4 μ initially to 1/2 μ at the end of the implosion. This frequency shaping was adjusted to achieve implosion symmetry while avoiding electron decoupling. Fifty kilojoules of laser energy was inputted and the hot electron spectra are assumed to be near Maxwellian. The pulse shape described earlier was modified to increase the symmetry and optimize the fusion yield. Figure 10 shows the two-dimensional Lagrangian mesh of a quadrant of the spherical pellet after implosion from 400 μ to about 100 μ. Errors in symmetry are less than one percent and Taylor instability growth is insignificant. The thermonuclear yield produced in this two-dimensional calculation was 1750 KJ, only a few percent less than that in the corresponding one-dimensional calculation. If it is assumed that the hot electron tails generated by plasma instabilities are unusually severe, it may be necessary to extend the frequency shaping to 1/4 μ light and to use hollow pellets.

A two-dimensional calculation was made of the same pellet in which the thickness of the initial atmosphere was reduced by a factor of two; only 1 μ light was used, and the pulse shape was not tailored to increase the symmetry. Severe asymmetries are evident. Figure 11. Negligible thermonuclear yield was produced because the axial perturbation reached the center before high temperatures and densities could be achieved.

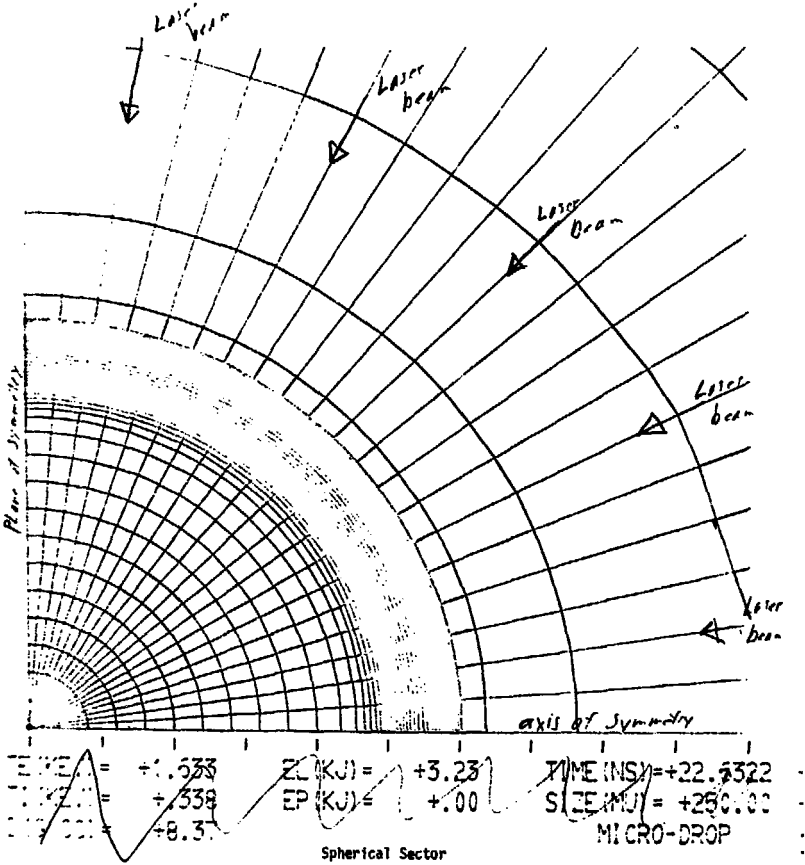

Spherical Sector

FIGURE 10
Two-Dimensional Implosion Calculation

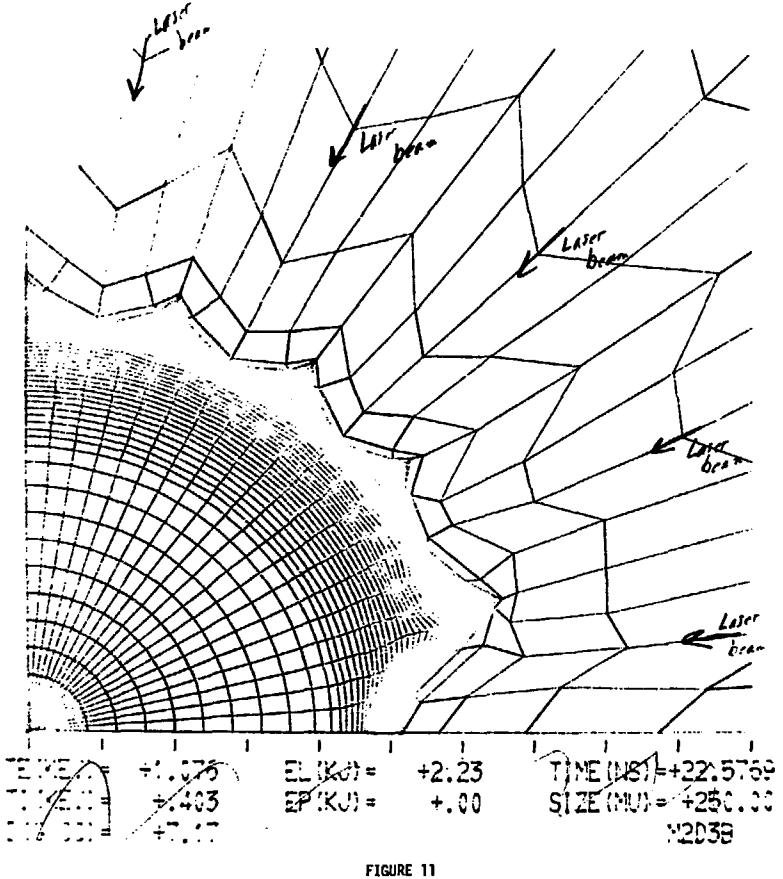

FIGURE 11

Two-dimensional implosion calculation--no frequency shaping, insufficient atmosphere.

CTR APPLICATION

Cheap fuel pellets are required for commercial power production. Ten million joules of electrical energy is currently worth roughly one cent, and most of this cent must be used to pay capital and operating costs of the power plant. In the scheme described here the pellet may be a droplet of DT (or deuterium, using multi-megajoule lasers) ejected from a sophisticated eye dropper and spherized by surface tension and viscosity effects, while freely falling in an evacuated drop tower. The pellet may also be a hollow sphere of fusion fuel. The high cost of tritium is obviated by regenerating the consumed tritium by means of neutron reactions in lithium blankets.

Thermonuclear microexplosions producing of the order of 10^7-10^8 joules (5-50 pounds TNT equivalent) may be suitable for commercial power production. Then multigigawatt-electric average power levels could be achieved by burning of the order of 100 pellets per second, perhaps 10 per second in each of 10 explosion chambers.

The electrical power, P, is related (via energy conservation) to the laser energy, L, explosion frequency, N, gain, G_L, and thermal-electric efficiency ϕ_L by

$$P = LN\,(G_L\,\phi_t - \phi_L^{-1})\ .$$

where it is assumed the laser is electrically pumped and the hot gas exhausted from the laser is not used to generate electricity. Less than one third of the electrical energy circulates internally if $G_L\,\phi_t \geq 3\,\phi_L^{-1}$.

Then if $\phi_t = 0.4$, $\phi_L = 0.1$, G_L must be 75 or more, which occurs for $L \sim 10^5$-10^6 joules--see Figure one. Then if $P = 10^9$ watts, $L = \frac{1}{2} \times 10^6$ joules and $N = 100\ sec^{-1}$.

The explosive impulse from a fusion energy pulse is much smaller than that from a chemical explosion of the same energy, because the fusion pellet weight is $< 10^{-6}$ that of the chemical, and the impulse generated is proportional to the square root of the mass. However, a specially designed combustion chamber is required to withstand the neutrons, x-rays, and hot plasma. A chamber several meters in diameter can be designed to withstand the neutron flux. The walls may be protected from x-rays and plasma by a thin film of Li[21].

Conventional thermal cycles may be used to generate electricity if the fusion neutrons are absorbed in lithium blankets. If relatively large DT pellets or essentially pure deuterium pellets are burned (requiring a multi-megajoule laser energy), the fusion neutrons will deposit much of their energy in the fuel plasma, and this plasma may be expanded against a magnetic field, and much of the fusion energy directly converted to electricity[22]. Then higher electrical generating efficiencies may be achieved. With deuterium pellet burning, lithium utilization and tritium storage and cycling may be greatly reduced.

Hybrid reactors--in which the 14 MeV DT neutrons which escape from the combustion chamber are used to fission natural uranium (or thorium)--may be capable of generating more energy than used to pump the laser even with low efficiency, low energy lasers (e.g. 1% efficient, 10 KJ lasers).

A high energy, high efficiency, short wavelength laser which is sufficiently cheap and capable of firing up to 100 times per second must be developed for CTR applications. This laser, the associated electrical

power source, and the explosion chamber must be designed to function up to 10^{10} times without replacement. The overall capital cost of this equipment must be less than about $100 per installed kilowatt (electrical). Although these are formidable technological problems, it is believed that they are soluble.

Acknowledgments

I would like to acknowledge important and useful discussions with S. Bodner, J. DeGroot, J. Katz, W. Kruer, A. Thiessen, G. Zimmerman, and particularly L. Wood.

REFERENCES

(1) J. Nuckolls, L. Wood, A. Thiessen, G. Zimmerman, Nature 239, 139, (1972).

(2) E. Teller, Science 121, 267 (1955).

(3) J. Nuckolls, et al., Livermore report UCRL-74116 (1972).

(4) J. Mayer, M. Mayer, Statistical Mechanics, Wiley (1940), p. 385.

(5) T. Weaver, G. Zimmerman, L. Wood, Livermore report UCRL-74191/ UCRL-74352 (1972).

(6) J. Shearer, UCRL-72400 (1970).

(7) W. Kruer, private communication.

(8) J. Katz, J. Weinstock, W. Kruer, J. DeGroot, R. Faehl, Livermore report UCRL-74334 (1972).

(9) R. Kidder, Physics of High Energy Density, (1969), Academic Press, p. 315.

(10) R. Kidder, J. Zink, Nucl. Fusion 12, 325 (1972).

(11) J. Stampen, et al., Phys. Rev. Lett. 26, 1012 (1971).

(12) S. Braginskii, Reviews of Plasma Physics 1, 205 (1965).

(13) L. Wood, et al., Livermore report UCRL-74115 (1972).

(14) G. Taylor, Proc. Royal Society 201A, 192 (1950).

(15) C. Leith, LLL internal report (1962).

(16) G. Zimmerman, Livermore report UCLR-50021-72-1, 107 (1972).

(17) D. Post, J. Wilson, LLL internal document (1972).

(18) W. Lokke, J. Ramus, LLL internal document (1972).

(19) J. Chang, G. Cooper, Jour. of Comp. Phys. 6, No. 1, 1 (1970).

(20) S. Bodner, Livermore report UCRL-74074 (1972).

(21) L. Booth, et al., Los Alamos report LA-4858-MS, Vol. 1 (1972).

(22) B. Freeman, L. Wood, J. Nuckolls, Livermore report UCRL-74486 (1971).